

# A Distributed Neural Linear Thompson Sampling Framework to Achieve URLLC in Industrial IoT

Francesco Pase, *Student Member, IEEE*, Marco Giordani, *Member, IEEE*, Sara Cavallero, *Student Member, IEEE*, Malte Schellmann, Josef Eichinger, Roberto Verdone, *Senior Member, IEEE*, Michele Zorzi, *Fellow, IEEE*

**Abstract**—Industrial Internet of Things (IIoT) networks will provide Ultra-Reliable Low-Latency Communication (URLLC) to support critical processes underlying the production chains. However, standard protocols for allocating wireless resources may not optimize the latency-reliability trade-off, especially for uplink communication. For example, centralized grant-based scheduling can ensure almost zero collisions, but introduces delays in the way resources are requested by the User Equipments (UEs) and granted by the gNB. In turn, distributed scheduling (e.g., based on random access), in which UEs autonomously choose the resources for transmission, may lead to potentially many collisions especially when the traffic increases. In this work we propose DIStributed combinatorial NEural linear Thompson Sampling (DISNETS), a novel scheduling framework that combines the best of the two worlds. By leveraging a feedback signal from the gNB and reinforcement learning, the UEs are trained to autonomously optimize their uplink transmissions by selecting the available resources to minimize the number of collisions, without additional message exchange to/from the gNB. DISNETS is a distributed, multi-agent adaptation of the Neural Linear Thompson Sampling (NLTS) algorithm, which has been further extended to admit multiple parallel actions. We demonstrate the superior performance of DISNETS in addressing URLLC in IIoT scenarios compared to other baselines.

**Index Terms**—Distributed scheduling; Multi-Armed Bandit; Thompson Sampling; Industrial Internet of Things (IIoT).

## I. INTRODUCTION

As 5th generation (5G) systems are already in the full implementation phase, the research community is now discussing future 6th generation (6G) networks and their requirements [1]. One of the driving forces in 6G is the design of new communication interfaces and architectures for Industrial Internet of Things (IIoT) networks, in which sensors, wearables, actuators, and robots are wirelessly interconnected in factories to enable analytics, diagnostics, monitoring, asset tracking, as well as process, regulatory, supervisory, and safety applications [2]–[4]. In this scenario, IIoT poses strict communication

requirements to achieve almost real-time coordination, control, and sensing [5]. Specifically, these requirements translate into latency (less than 1 ms in the radio part) and reliability (up to 99.99999%) constraints, thus calling for Ultra-Reliable Low-Latency Communication (URLLC) [6], [7].

As far as latency is concerned, the time introduced by Radio Access Network (RAN) operations, from routing and resource allocation to modulation, represents one of the most significant sources of delay. In particular, the Controller/Master (C/M), i.e., the Next Generation Node B (gNB) of the IIoT network, should be able to provide almost immediate channel access to User Equipments (UEs) in the factory floor, ideally as soon as they have data to send. This is especially critical for uplink communication, as additional energy and computational constraints at the end nodes may further delay the time it takes to access the channel [8], [9].

However, the 5G standard is unlikely to provide resource allocation in short time, mainly due to the intrinsic limitations of current channel access schemes [10], [11]. Notably, the 3rd Generation Partnership Project (3GPP) New Radio (NR) specifications for 5G networks [12] support three options to allocate uplink resources: grant-based scheduling (GBS), semi-persistent scheduling (SPS),<sup>1</sup> and grant-free scheduling (GFS) [14]. GBS [15] is fully centralized, and requires: (i) the UEs to use the Physical Uplink Control Channel (PUCCH) to ask the uplink scheduler for being scheduled; (ii) the gNB to communicate via the Physical Downlink Control Channel (PDCCH) to the UEs which resources can be used for transmission; (iii) the UEs to transmit their data blocks through the Physical Uplink Shared Channel (PUSCH); and (iv) the gNB to provide the communication acknowledgment via Hybrid Automatic Repeat reQuest (HARQ). This procedure requires at least two Round Trip Times (RTTs) from when data arrives in the buffer until it can be properly scheduled, which may prohibitively increase the communication delay. SPS [16] is also fully centralized, but permits the gNB to pre-allocate radio resources without explicit scheduling requests and grants from/to the UEs, thus reducing the latency. However, the periodicity of scheduling grants is defined by Radio Resource Control (RRC) signaling at the session establishment based on the predicted traffic at the UEs, and may cause large and systematic delays in case of errors in those predictions. On the other extreme, GFS [17] is fully distributed, and

Francesco Pase, Marco Giordani, and Michele Zorzi are with WiLab and the Department of Information Engineering (DEI) of the University of Padova, Italy. Email: {pasefrance,giordani,zorzi}@dei.unipd.it.

Sara Cavallero, and Roberto Verdone are with WiLab and Dipartimento di Ingegneria dell'Energia Elettrica e dell'Informazione "Guglielmo Marconi" of the University of Bologna, Italy. Email: {s.cavallero,roberto.verdone}@unibo.it.

Josef Eichinger and Malte Schellmann are with Huawei Technologies, Munich Research Center, Germany. Email: {joseph.eichinger,malte.schellmann}@huawei.com.

This work has been carried out in the framework of the CNIT National Laboratory WiLab and the WiLab-Huawei Joint Innovation Center. This work was also partially supported by the European Union under the Italian National Recovery and Resilience Plan (NRRP) of NextGenerationEU, partnership on "Telecommunications of the Future" (PE0000001 - program "RESTART").

<sup>1</sup>Formally, 3GPP 5G NR specifications define SPS for downlink scheduling, and Configured Grant (CG) Type 1 and Type 2 for uplink scheduling, where Type 2 is similar to SPS with minor modifications [13]. For simplicity, in the remainder of this paper we will refer to SPS also for uplink scheduling, even though our implementation is based on CG Type 2 specifications.

the UEs autonomously choose radio resources to be used for transmission, thereby eliminating the need to wait for scheduling grants. On the downside, uncoordinated resource allocation may lead to collisions, and trigger re-transmissions accordingly, which again pose additional latency concerns.

In this context, machine learning (ML) has emerged as a promising tool to optimize network performance, including minimizing latency during resource allocation. Still, most of the literature focuses on centralized and downlink algorithms, e.g., [18], which however are not scalable as the density of the network increases. In the area of distributed learning, Multi-Armed Bandit (MAB) algorithms [19], and especially Linear Thompson Sampling (LTS) [20], gained popularity to address the problem of resource allocation. However, these schemes are often too simple to model complex network dynamics, and work with the assumption of linear dependency of data [21]. A promising attempt to overcome this limitation was made with the Neural Linear Thompson Sampling (NLTS) algorithm [22], which still assumes that the ML agent can only play single actions, i.e., UEs transmit through one single orthogonal channel, which may increase the latency beyond URLLC requirements.

#### A. Contributions

To solve these issues, in this work we propose a new distributed framework for resource allocation called DIStributed combinatorial NEural linear Thompson Sampling (DISNETS), which is built upon two cardinal principles. First, it consists of a UE-centric architecture in which resource allocation decisions are made by the local UEs, “disaggregated” from the network, and without pre-defined scheduling requests and/or grants. Second, UEs rely on ML to optimize resource allocation, which allows to minimize the probability of collisions and reduce the latency due to re-transmissions. To this aim, our contributions are the following:

- We formalize the problem of distributed resource allocation as a Multi-Agent Contextual Combinatorial Multi-Armed Bandit (MA-CC-MAB) problem, where UEs autonomously choose the physical resources to use for transmission. The problem is solved using DISNETS, built on top of the NLTS algorithm [22], which combines Deep Neural Network (DNN) and LTS to optimize network operations. Specifically, the original NLTS implementation is extended into the proposed DISNETS solution by allowing agents to take more than one action at each scheduling opportunity, i.e., using multiple orthogonal channels in parallel in the same scheduling opportunity, which is important to provide URLLC.
- We propose the design and structure of a new control signaling scheme, referred to as Feedback Control Information (FCI), and used by the UEs to train and learn how to allocate resources using DISNETS. The structure of the FCI is similar to that of the Downlink Control Information (DCI) signal, which is currently used in 5G NR to enable centralized scheduling [23].
- We apply DISNETS to the context of URLLC in IIoT environments. As such, we propose a new ad hoc traffic model in which industrial machines and users in a production line activate and generate traffic, respectively, based

on some temporal and spatial correlations. This approach promotes more realistic, IIoT-specific simulations.

- We validate DISNETS through end-to-end (E2E) simulations in terms of latency and reliability, against 5G NR GBS and SPS baselines for resource allocation, and GFS based on random access. Simulation results are given as a function of the number of UEs in the network, the traffic configuration, and some other IIoT-specific system parameters. We show that DISNETS achieves faster and more accurate resource allocation than its competitors, also in the presence of aperiodic and unpredictable traffic.

#### B. Paper Organization

The rest of the paper is organized as follows. After discussing some related work in Sec. II, in Sec. III we describe our system model, in Sec. IV we present our MA-CC-MAB problem formulation, in Sec. V we solve the problem using the proposed DISNETS algorithm, in Sec. VI we provide numerical results, and in Sec. VII we summarize our main conclusions and suggestions for future research.

## II. RELATED WORK

Achieving URLLC has been a long-standing research problem, motivated by the several services, applications, and verticals that pose stringent networking requirements [24]. Adaptive modulation and coding schemes, short-length packet coding, channel access and re-transmission, and resource allocation are just a few examples of network operations that need to be optimized to achieve URLLC [25]. Notably, as highlighted in [11], [21], [26], resource allocation currently represents the bottleneck to reduce the latency below 1 ms. This is mainly due to the current limitations of standard resource allocation protocols, which cannot dynamically and proactively trade off low latency and high reliability [23], especially for uplink communication [11]. On one hand, centralized GBS and SPS can coordinate the allocation of physical resources to minimize the number of collisions, but imply some sort of communication between the UEs and the gNB to agree on the resources to use before sending data [11]. On the other hand, distributed GFS protocols, in which the UEs can autonomously choose the physical resources for uplink communication without grants, can eliminate a good part of the delay. However, this option naturally leads to higher collisions probability as many UEs may utilize the same wireless resources given the lack of coordination, which may prevent URLLC in dense networks [17].

Along these lines, the literature has proposed many solutions to optimize the system performance beyond model-based architectures, especially using ML models trained on network data [27], [28]. The general idea is to formulate the problem as a decision-making process, and to carefully design a feedback signal rewarding the agent as some network metrics (e.g., latency, reliability, fairness, power consumption, and so on) are satisfied. For example, the authors in [18] expressed the problem of resource allocation for URLLC as a Markov Decision Process (MDP), and solved it through Deep Reinforcement Learning (DRL). In [29], the authors introduced prior knowledge into the system, and showed that

this approach can reduce the convergence time of the DRL solution. However, these works focus on downlink traffic with centralized scheduling, which is usually not scalable as the number of UEs increases.

To target this problem, the research community has studied distributed multi-agent MDP [30], which allows the UEs, i.e., the agents, to make autonomous decisions on the physical resource(s) to use for communication without the support from an external centralized entity [21]. For instance, in [31] the authors used game theory to define and study the performance of distributed resource allocation in which each agent is trained to select physical resources so as to avoid collisions. However, the problem was considerably simplified to be mathematically tractable, and no simulations on real communication systems have been performed. In our recent paper [21] we also proposed a similar formulation, in which four state-of-the-art MAB algorithms have been compared to identify the best implementation in terms of latency and reliability. The analysis suggested that the Thompson Sampling (TS) algorithm is a good candidate, achieving zero collisions in our experiments. However, the system model in [21] was quite simple, and most importantly each agent was designed to select only one orthogonal resource to transmit data, which is not realistic in practice. In [32], the authors developed a similar framework to manage distributed Vehicle-To-Everything (V2X) communication without relying on global information. In this case, each UE was equipped with a DRL agent, which is more complex and difficult to handle than MAB but potentially offers more flexibility and better performance. However, each agent could still choose only one physical resource per scheduling opportunity, as choosing more would have increased exponentially the action space, so the complexity.

Based on the above introduction, in this work we decided to formulate the problem of distributed resource allocation as an MA-CC-MAB problem [19], which generally achieves faster convergence than multi-agent DRL. The MA-CC-MAB problem is solved using DISNETS, which combines and extends the LTS [20] and NLTS [22] algorithms so that agents can use (and are trained to choose) multiple orthogonal resources in the same scheduling unit, in the hope to transmit data faster. We will demonstrate in Sec. VI that this approach outperforms state-of-the-art centralized and decentralized benchmarks.

### III. SYSTEM MODEL

In this section we present our system model. Specifically, we describe our factory layout and scenario in Sec. III-A, the channel model in Sec. III-B, the traffic model to characterize IIoT-specific interactions between machines, end users, and the underlying factory geometry and functionalities in Sec. III-C, and the E2E latency and reliability models in Sec. III-D.

#### A. Scenario

*a) Factory floor:* We consider a limited geographical area within an indoor factory floor, modeled as a parallelepiped of length  $l$ , width  $w$ , and height  $h$ , as reported in [33]. Then,  $M$  industrial machines are grouped into  $W$  different production lines (each of which models an underlying industrial process), and are connected to a Standalone Non-Public Network (SNPN), i.e., a 5G remote and private network

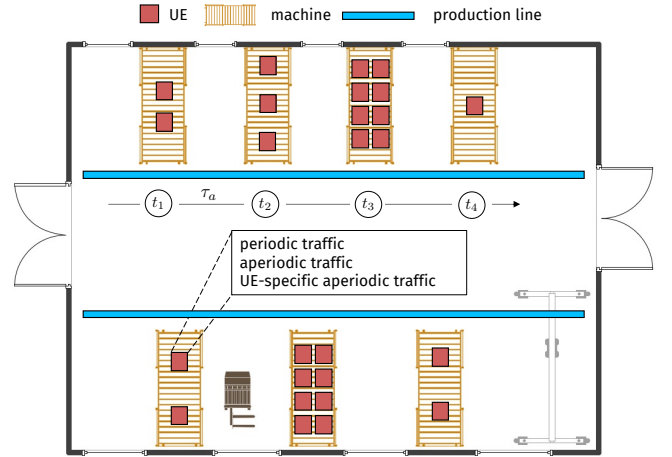


Fig. 1: Factory floor layout (with  $W = 2$ ,  $M = 7$ , and  $N = 18$ ) and traffic correlation. Specifically, machines in each production line are correlated, and activate according to a specific sequence on the production line, i.e., toward the right or the left. At  $t_1$ ,  $W = 2$  machines (i.e., one per production line) activate, and the corresponding UEs onboard the active machines start sending data as periodic, aperiodic, or UE-specific aperiodic traffic. At  $t_2 = t_1 + \tau_a$ , these machines shut down and the next activation begins.

with a reserved RAN and 5G Core (5GC) [34]. For example, Fig. 1 illustrates an example with  $W = 2$  production lines and  $M = 7$  machines. Machines are modeled as cubes of size  $S$ , and deployed across the factory floor according to a uniform distribution, ensuring a given inter-machine distance  $D$  between the centers of the machines. Onboard the machines,  $N$  UEs are distributed following the same method, at a maximum height  $S$ , and generate traffic according to predefined patterns (see Sec. III-C). Moreover, obstacles act as obstructions between the UEs and the gNB.

*b) Resource allocation:* We consider uplink communication, i.e., from the  $N$  UEs to the C/M, that is a remote entity monitoring and controlling the machines from the 5GC through a gNB. The total available bandwidth  $B$  is split into  $K$  orthogonal channels where, according to the 3GPP nomenclature, an orthogonal channel consists of 12 Orthogonal Frequency Division Multiplexing (OFDM) subcarriers. Time is also discretized into Scheduling Units (SUs) whose duration is of 7 OFDM symbols. Then, a Resource Block (RB) is defined as the minimum physical resource unit that can be allocated for data transmission, and consists of one orthogonal channel in frequency, and one SU in time. Within one SU, the first 4 OFDM symbols are dedicated to the PUSCH used by the UEs to transmit data, and the last 2 OFDM symbols are used by the gNB to convey the FCI, as described in Sec. V-A.

*c) Data transmission:* Whenever a UE has new data packets to send, it can use multiple RBs choosing different orthogonal channels within the same SU. The assumption in our system model is that, whenever two or more UEs use the same orthogonal channels in the same SU, i.e., the same set of RBs, they create a collision, and we assume all data packets to be lost, i.e., they cannot be detected by the gNB.

#### B. Channel Model

The channel is characterized based on the Indoor Factory (InF) model for IIoT networks [35, Table 7.2-4]. Specifically,

the 3GPP identifies several InF scenarios depending on the density of obstacles and the location of the UEs with respect to the gNB. Among these, in this paper we selected the most representative 3GPP InF scenario based on the 5G-ACIA factory layout and geometry described in [34] and Sec. III-A.

The path loss depends on the Line of Sight (LOS) or Non-Line-of-Sight (NLOS) condition of the channel. In this regard, the 3GPP provides an expression for the LOS probability in [35]. However, we do not adopt a statistical model to discriminate between LOS and NLOS propagation. On the contrary, we implement a geometry-based approach that checks whether the joining line between the UE's and the gNB's centers intersects one or more obstacles. If so, the UE is considered in NLOS, otherwise it is in LOS. Then, the quality of the received signal is assessed in terms of the Signal-to-Noise-Ratio (SNR), which is defined as

$$\text{SNR} = \frac{P_{\text{TX}} \cdot G_{\text{UE}} \cdot G_{\text{gNB}}}{PL \cdot P_N}, \quad (1)$$

where  $P_{\text{TX}}$  is the transmit power,  $G_{\text{UE}}$  and  $G_{\text{gNB}}$  are the antenna gains at the UE and the gNB, respectively,  $PL$  is the path loss, and  $P_N$  is the Additive White Gaussian Noise (AWGN) power. The latter is computed as  $k_B \cdot T \cdot B$ , where  $k_B$  is the Boltzmann constant,  $T$  is the system noise temperature (in K), and  $B$  is the total bandwidth (in Hz) at the gNB. The SNR is used to check whether a data block is correctly decoded, i.e., if the SNR is above a given threshold  $\text{SNR}_{\text{th}}$ , and to determine the modulation order to be used for data transmission according to [36].

### C. The Spatio-Temporal Correlated Traffic Model

In most of the literature, uplink traffic is assumed either periodic (i.e., UEs generate data at predefined time intervals) or totally aperiodic (i.e., UEs generate data at random intervals), and machines in the factory floor can generate packets simultaneously. In this paper, we propose an alternative traffic model where data packets are generated according to predefined statistics, to better characterize IIoT interactions. In this model, machines within a production line are sequentially activated, emulating the workflow of the corresponding industrial process. Then, UEs onboard active machines produce data traffic (either periodic or aperiodic [37]) for an entire "activation period" of duration  $\tau_a$ , after which another machine in the current production line will activate.

As such, the traffic model accounts for both spatial and temporal correlation, as illustrated in Fig. 1. Notably, it is possible to identify two different types of correlation.

a) *Inter-machine correlation*: It refers to the way machines activate. Specifically, when an event occurs, one machine per production line is activated. Then, after the activation period, the next machine activates following the flow of the production line, at a sequence that depends on the factory geometry and the number of machines and lines.

b) *Intra-machine correlation*: It refers to the way UEs onboard the active machines generate packets. After one machine per line is activated, the UEs associated with those machines activate too. Then, active UEs generate a flow of packets according to some statistics, e.g., in terms of the

inter-packet interval and/or the packet size, until some new machines in the production line activate. We consider:

- *Periodic traffic*, if packets are generated at constant periodicity  $\tau$  [37]. For example, UEs periodically measure and report physical parameters (e.g., temperature, pressure, radiation) from the production process.
- *Uniformly aperiodic traffic*, if the inter-packet interval  $\tau$  is modeled as a uniform random variable in  $[t_{\min}, t_{\max}]$ . For example, UEs make unscheduled aperiodic transmissions in case abnormal measurements are detected.
- *UE-specific aperiodic traffic*, in which the extreme values  $t_{\min}$  and  $t_{\max}$  are UE-dependent parameters. Specifically, we now assume that  $\text{UE}_n, \forall n \in \mathcal{N}$ , where  $\mathcal{N}$  is the set of UEs, generates with probability one another packet in the interval  $[t_{\min}^n, t_{\max}^n]$ , with  $t_{\min}^n$  and  $t_{\max}^n$  modeled as uniform random variables within the intervals  $[t_{\min}, t_{\max}]$  and  $[t_{\min}^n, t_{\max}^n]$ , respectively. Notably, we now have  $t_{\min} \leq t_{\min}^n \leq t_{\max}^n \leq t_{\max}$ . The rationale behind this new traffic model is that, in real-world factories, some sensors/UEs may control different parts or mechanisms of the same inter-machine process, thus activating with statistics that depend on their roles or position, and so are UE-specific.

### D. Latency and Reliability Models

a) *Latency*: We require our system to minimize the E2E latency in uplink, which is defined as the time from when one packet is generated at the UE's application to when the same packet is successfully received by the C/M. Specifically, the E2E latency  $L$  of a packet is computed as:

$$L = T_P + T_{\text{RAN}} + T_{\text{TX}} + \tau_P + T_{\text{DAS}} + \tau_F + T_{\text{gNB}} + T_{\text{CN}}, \quad (2)$$

where, based on the analysis in [11]:

- $T_P$  is the time for the UE to create the data packet, i.e., to add headers across the 5G protocol stack;
- $T_{\text{RAN}}$  is the time between the generation of the data packet at the Physical (PHY) layer and the packet transmission, which depends on the scheduling algorithm;
- $T_{\text{TX}}$  is the transmission time;
- $\tau_P$  is the propagation time from the UE to the fronthaul of the gNB, i.e., the Distributed Antenna System (DAS);
- $T_{\text{DAS}}$  is the time for the DAS to process the received data packet, and to send it to the gNB;
- $\tau_F$  is the time for the signal to travel from the DAS to the gNB, generally through a high-capacity optical fiber;
- $T_{\text{gNB}}$  is the time for the gNB to process the received data block, and to send it to the C/M;
- $T_{\text{CN}}$  is the delay introduced by the 5GC, that is the time for the message to reach the C/M from the gNB.

Finally, we denote as  $\bar{L}$  the average E2E latency, averaged over the data packets generated by the UEs within the simulation time  $T_S$ , and over the number of UEs.

b) *Reliability*: We also require our system to operate with high reliability. We define a reliability metric  $\eta_t(L_{\text{th}})$  as the empirical probability that the E2E latency of a packet is below a pre-defined threshold  $L_{\text{th}}$  during  $\text{SU}_t$ , and  $\bar{\eta}_t(L_{\text{th}})$  is the empirical average of  $\eta_t(L_{\text{th}})$  within the simulation time  $T_S$ .

#### IV. PROBLEM FORMULATION

The aim of our work is to minimize  $T_{\text{RAN}}$  in Eq. (2), which dominates the E2E latency, and depends on the underlying resource allocation procedure. As mentioned in Sec. I, standard 5G NR protocols mainly adopt either centralized scheduling at the gNB (i.e., GBS and SPS), which introduces delays due to the rigidity of the resource allocation scheme with respect to the traffic generation process, or distributed scheduling (i.e., GFS), which may result in collisions. In turn, we propose DISNETS, a new scheduling framework that combines the benefits of the two: on one side, resource allocation is decentralized, in the sense that UEs autonomously decide how to allocate resources without significant interactions with the gNB, which eliminates the waiting time to receive scheduling grants; at the same time, UEs exploit ML to optimize scheduling decisions based on traffic correlations, which may reduce the probability of collision. Our research problem is formulated as a MA-CC-MAB problem, as described below.

##### A. The CC-MAB Problem

The problem formulation is built on top of the Contextual Combinatorial Multi-Armed Bandit (CC-MAB) framework [38]. Specifically, every time UE $_n \in \mathcal{N}$ , i.e., an agent, has data to send in SU $_t$ , it will autonomously choose the physical resources to be used for transmission. The total available bandwidth is split into  $K$  orthogonal channels, and we denote with  $\mathcal{K} = \{1, 2, \dots, K\}$  the set of channels. In CC-MAB parlance, the  $K$  orthogonal channels are the  $K$  feasible actions that can be chosen by the agent. To take an action, each agent can rely on side information (i.e., the context  $s_t \in \mathcal{S}$ ) that describes the state of the environment (i.e., the wireless network) in SU $_t$ , which we model as a random variable sampled according to the system's probability  $P_S$ . Given the context  $s_t$  and the action  $k_t$  chosen by the agent in SU $_t$ , the environment returns a reward  $r_t \in [-1, 1]$  according to the probability  $P_R(s_t, k_t)$ , which reflects the probability that data transmission using channel  $k_t$  in context  $s_t$  was successful. Specifically,  $r_t = -1$  if collisions happen, otherwise it is proportional to the number of transmitted bits (see Eq. (9) for further details). Then,  $\mu(s, k)$  is the average reward with respect to the distribution  $P_R(s, k) \forall s \in \mathcal{S}, \forall k \in \mathcal{K}$ .

In our framework, the CC-MAB problem is extended by allowing agents to take more than one action in each SU, i.e., using multiple orthogonal channels in parallel in the same SU, which is important to provide URLLC. Therefore, we define a super-action  $\theta_t \subset \mathcal{K}$  as a set of actions in SU $_t$ , so  $\theta_t$  is an element of the super-set  $\Theta$  of  $\mathcal{K}$ , i.e., the set of all possible subsets of  $\mathcal{K}$ . The reward  $r_t$  is then sampled according to  $P_R(s_t, \theta_t)$ . Interestingly, we can exploit the structure of the environment to assume that

$$\mu(s, \theta) \sim \sum_{k \in \theta} \mu(s, k), \quad \forall s \in \mathcal{S}, \theta \subset \mathcal{K}, \quad (3)$$

i.e., the average reward relative to super-action  $\theta$  is proportional to the sum of the average rewards of the single actions.

To choose the super-action in SU $_t$ , the agent employs a policy  $\pi_t : \mathcal{H}^{t-1} \times \mathcal{S} \rightarrow \Phi(\Theta)$ , which is a map from the history  $H_t = \{(s_1, \theta_1, r_1), \dots, (s_{t-1}, \theta_{t-1}, r_{t-1})\} \in \mathcal{H}^{t-1}$

of previous contexts, actions, and rewards, to a probability distribution over the set of feasible super-actions  $\Theta$ . Given a horizon  $T$ , the goal of the agent is to find the policy  $\pi^*$  that maximizes the expected sum of rewards over time, i.e.,

$$\pi^* = \arg \max_{\pi} \mathbb{E} \left[ \sum_{t=1}^T \mu(s_t, \theta_t) \right], \quad (4)$$

where the expectation is taken with respect to the distributions of  $P_R$  and  $P_S$  and the agent's policy  $\pi_t$ , used to sample super-actions according to  $\theta_t \sim \pi_t(s_t)$ .

##### B. The MA-CC-MAB Problem

In our work we further extend the CC-MAB problem in Sec. IV-A, and formulate a new MA-CC-MAB problem where the reward depends on the other agents' actions in SU $_t$ . Therefore, the reward  $r_{n,t}$ , the context  $s_{n,t} \in \mathcal{S}_n$ , and the policy  $\pi_{n,t}$  at time  $t$  are now a function of the agent  $n$ . This is critical to support more accurate distributed resource allocation, where there is no or little interaction among the UEs.

A collision event is expressed by the random variable  $\chi(k, t) \in \{0, 1\}$ , which is equal to 1 when collision(s) happen in the orthogonal channel  $k$  in SU $_t$ , and 0 otherwise. As such, it is modeled by each agent as a Bernoulli random variable of parameter  $\varphi(s_{n,t})$ .<sup>2</sup> By modeling assumption, whenever two agents  $n$  and  $n'$  play super-actions  $\theta_{n,t}$  and  $\theta_{n',t}$ , respectively, we have that  $\chi(k, t) = 1, \forall s \in \mathcal{S}$ , if  $k \in \theta_{n,t} \cap \theta_{n',t}$ , as collisions occur. Notice that agents make decisions based only on local data, so that agent  $n$  does not know a priori the structure of vectors  $\theta_{n',t}, n' \neq n$ . As such, agents can just rely on the local context  $s_{n,t}$ , and the statistical knowledge acquired through history  $H_{n,t}$ .

#### V. PROPOSED SOLUTION: THE DISNETS FRAMEWORK

In this section, we present the proposed solution to the MA-CC-MAB problem introduced in Sec. IV-B. The proposed framework implements (i) a new control signal called FCI (Sec. V-A), which conveys the information to compute the reward  $r_{n,t}$  and is used to generate the context  $s_{n,t}$ , and (ii) the DISNETS algorithm (Sec. V-B), which combines LTS and NLTS to solve Eq. (4), and allows end users to autonomously allocate resources for uplink transmissions.

##### A. Context and FCI Implementation

As introduced in Sec. IV-A, the agents optimize policies  $\pi_{n,t}$  based on the rewards  $r_{n,t}, \forall n \in \mathcal{N}$ . In our framework, the reward is based on the new FCI signal depicted in Fig. 2, which has a similar structure as the 5G NR DCI signal. The FCI, sent from the gNB to the UEs, is located in the last 2 OFDM symbols of each SU, and includes the transmission outcomes in that SU relative to each orthogonal channel. Based on the received power on each orthogonal channel, the gNB can distinguish among four outcomes, namely successful

<sup>2</sup>Notice that  $\chi(k, t)$  does not explicitly depend on  $n$  but has the same value for all the agents. In turn, its statistics, specifically  $\varphi(s_{n,t})$ , are modeled using the local context  $s_{n,t}$  as agents have missing information on the other agents' actions.

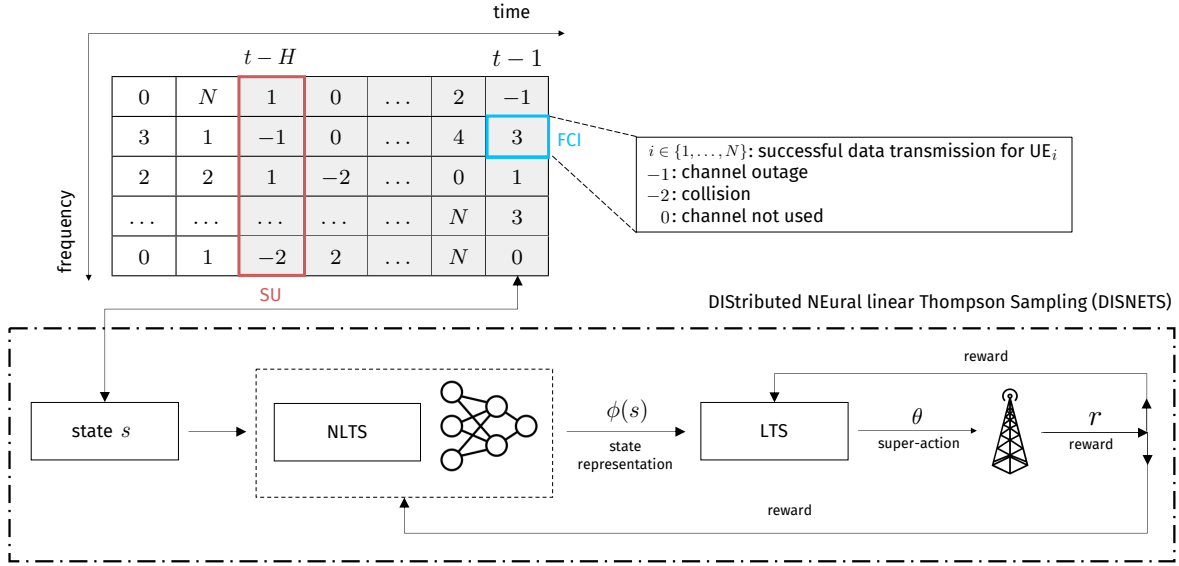


Fig. 2: Schematic representation of DISNETS. The framework consists of (i) the state/context  $s$ , (ii) an NLTS module to provide the non-linear representation of the context  $\phi_\omega(s)$ , (iii) an LTS module to choose a super-action  $\theta \in \mathcal{K}$  corresponding to the set of orthogonal channels to use to transmit data, (iv) the reward  $r$  (incorporated within the FCI) to update the NLTS and LTS parameters.

transmission for UE<sub>*i*</sub> (FCI =  $i$ ,  $i \in \{1, \dots, N\}$ ), outage (FCI =  $-1$ ), collision (FCI =  $-2$ ), or channel not used (FCI =  $0$ ).

Based on the FCI, the UEs can compute their local contexts  $s_{n,t}$ ,  $\forall n \in \mathcal{N}$ , which are used to statistically describe the state of the system in  $SU_t$ . Specifically, the context  $s_{n,t}$  aggregates the outcomes from  $H$  previous FCI signals, which provides a history of previous resource allocation decisions.

### B. DISNETS Implementation

In this section we describe our DISNETS framework, represented in Fig. 2, to solve the MA-CC-MAB and support distributed resource allocation. DISNETS extends the NLTS algorithm, which is in turn based on the LTS algorithm.

*Notation.* For simplicity, we drop subscript  $n$ , with  $n \in \{1, \dots, N\}$ , to represent the index of the agent/UE.

a) *Linear Thompson Sampling (LTS):* DISNETS is built on top of the LTS algorithm [39] to choose an action  $k \in \mathcal{K}$ , which returns the orthogonal channel that the UE can use to transmit data. LTS assumes that the average reward behind each action  $k \in \mathcal{K}$  is a linear function of the context  $s_t \in \mathcal{S}$ , and of an unknown action parameter vector  $\beta_k$ , i.e.,  $\mu(s, k) = \langle s, \beta_k \rangle$ . In this case, estimating the most accurate vector  $\beta_k$ ,  $\forall k \in \mathcal{K}$ , turns out to be an online linear regression problem. The problem is online because the target values, i.e., the rewards associated to the pair  $(s, \beta_k)$ , are observed by the agent as it interacts with the environment and takes actions, respectively, and are not available at the beginning of the training process like in supervised learning.

To solve this online problem, LTS assumes that the rewards, given the context  $s$  and action  $k$ , are modeled as a Gaussian random variable<sup>3</sup>  $R(s, k)$ , i.e.,  $R(s, k) \sim \mathcal{N}(s^T \beta_k, \nu_k^2)$ . The LTS algorithm maintains a distribution of the parameter vector

of each action  $k$  at time  $t$ , i.e.,  $\beta_k(t)$ . Therefore  $P(\beta_k(t)) \propto \mathcal{N}(\hat{\beta}_k(t), \nu_k^2(\Phi_k(0) + \Phi_k(t))^{-1})$ , where

$$\Phi_k(0) = \lambda \cdot I_d; \quad (5)$$

$$\Phi_k(t) = \sum_{\tau=1}^{t-1} s_\tau s_\tau^T \cdot \mathbf{1}_{k_t=k}; \quad (6)$$

$$\hat{\beta}_k(t) = (\Phi_k(0) + \Phi_k(t))^{-1} \sum_{\tau=1}^{t-1} s_\tau r_\tau \cdot \mathbf{1}_{k_t=a}. \quad (7)$$

In particular,  $\lambda$  is a hyper-parameter governing the initial exploration,  $I_d$  is the identity matrix of size  $d$ , and  $\mathbf{1}_{k_t=k}$  is the indicator function and is equal to 1 if  $k_t = k$  or 0 otherwise. After observing context  $s_t$  and taking action  $k_t$ , the agent receives a reward  $r_t$  based on the FCI (Sec. V-A), and updates the distribution of the parameter vector at  $t+1$  as

$$\begin{aligned} & P(\beta_k(t+1)|s_t, r_t) \\ & \propto P(r_t|s_t, \beta_k(t+1)) \cdot P(\beta_k(t+1)) \\ & \propto \mathcal{N}(\hat{\beta}_k(t+1), \nu_k^2(\Phi_k(0) + \Phi_k(t+1))^{-1}). \end{aligned} \quad (8)$$

Based on the posterior update rule in Eq. (8), the agent samples  $K$  vectors  $\hat{\beta}_k$ ,  $\forall k \in \mathcal{K}$ , and plays action  $k_t = \arg \max_{k \in \mathcal{K}} \langle s_t, \hat{\beta}_k \rangle$ . The interesting property of LTS is that it balances *exploration*, i.e., sampling random actions to explore their reward statistics, and *exploitation*, i.e., exploiting the knowledge collected in previous time slots to optimize future decisions, and presents good empirical performance [21].

#### Summary : LTS

*Objective.* Choose an action  $k \in \mathcal{K}$ , and return the orthogonal channel that a UE should use to transmit data.  
*Problem.* It works under the assumption of linear dependency between the context and the average reward obtained by playing action  $k \in \mathcal{K}$ .

<sup>3</sup>According to [39], the rewards are not required to be Gaussian to converge to the optimal actions, but their domains need to be bounded.

---

**Algorithm 1: Neural Linear Thompson Sampling**

---

```

1 Initialize  $\Phi_k(0) = \lambda \cdot I_d, \hat{\beta}_k(0) = \beta_k(0) = 0, \psi_k = 0$ 
2 foreach  $t \in 1, \dots, T$  do
3   Observe  $s_t$  and compute  $z_t = \phi_\omega(s_t)$ 
4   Sample w.r.t  $\nu_k(t), \forall k \in \mathcal{K}$ , from  $\text{IG}(a_k(t), b_k(t))$ 
5   Sample w.r.t  $\beta_k, \forall k \in \mathcal{K}$ , from
      $\mathcal{N}(\hat{\beta}_k(t), \nu_k^2 (\Phi_k(0) + \Phi_k(t))^{-1})$ 
6   Play  $k_t = \arg \max_{k \in \mathcal{K}} z_t^T \beta_k$ 
7   Observe  $r_t$  and store  $(s_t, k_t, r_t)$  in the buffer
8   Update action posterior (Eq. (8)), using context  $z_t$ 
9   Update noise posterior
10  if  $\text{mod}(t, O) = 0$  then
11    Train  $f_\omega$  with SGD using samples in the buffer
12    Compute new  $z_t$ , and update LTS

```

---

*b) Neural Linear Thompson Sampling (NLTS):* As discussed in the previous paragraph, LTS assumes a linear relation between the context and the average reward obtained by playing one specific action. However, linear relations are not complex enough to model real-world scenarios. This problem is usually solved using DRL, which requires a long training phase. On the other hand, DNNs are potentially good candidates to model the many different relations between contexts and actions. On the downside, when using DNNs there are no closed form solutions for the posterior updates, like the one in Eq. (8). As such, different approximate solutions have been proposed in the literature.

In particular, the authors in [22] introduced a new algorithm, called NLTS, that models the non-linearity between contexts and rewards by assuming that the average reward  $\mu(s, k)$  is equal to a linear combination of the action parameter vector  $\beta_k$  and a non-linear representation of the context  $\phi(s)$ , i.e.,  $\mu(s, k) = \langle \phi(s), \beta_k \rangle$ . To do so, a DNN  $f_\omega(s): \mathcal{S} \rightarrow \mathcal{R}^K$ , parameterized by the weights vector  $\omega \in \Omega$ , is trained to estimate the average reward for each action, where  $\mathcal{R}$  is the range of the actions' reward, assumed to be the same for all actions. The non-linear representation of the context  $\phi(s)$ , or  $\phi_\omega(s)$  to illustrate the dependency on  $\omega$ , is the output of the last hidden layer of the DNN, i.e., the input of the last layer, whose output is  $f_\omega(s)$ . Then, NLTS uses LTS to choose the orthogonal channel for the UEs to transmit data, working on the state representation  $\phi_\omega(s)$  in place of  $s$ .

We highlight that the posteriors of LTS are updated based on Eq. (8) every time the agent makes a decision, while the parameters  $\omega$  of the DNN are updated at fixed intervals of  $O$  steps.<sup>4</sup> Another feature introduced by NLTS is that the distribution of the noise variance of the reward  $\nu_k$  is modeled using the Inverse Gamma distribution, i.e.,  $\nu_k(t) \sim \text{IG}(a_k(t), b_k(t))$ . The pseudocode of NLTS is reported in Algorithm 1.

<sup>4</sup>It is important to properly balance the optimization steps of the LTS module (performed at each interaction with the environment) and that of the NLTS module (performed every  $O$  interactions with the environment) of DISNETS to avoid training instabilities, as one module depends on the other.

**Summary : NLTS**

*Objective.* Compute the non-linear representation of the context  $\phi_\omega(s)$ , i.e., the output of the last hidden layer of the DNN, and use LTS to choose an action  $k \in \mathcal{K}$ , which returns the orthogonal channel that each UE should use to transmit data.

*Problem.* The agent can only play single actions, i.e., each UE can transmit through one orthogonal channel.

*c) DISNETS (Proposed):* As mentioned, we now enhance the NLTS algorithm to allow each agent to choose multiple actions, i.e., to use multiple orthogonal channels in the same SU as expected in real systems, which defines the MA-CC-MAB problem in Sec. IV-B. Intuitively, there are two main issues when applying basic NLTS to MA-CC-MAB: first, the super-action  $\theta$  that maximizes the expected reward  $\mu(s, \theta)$  is unknown a priori, as the effects of single actions can be combined in different ways to obtain the super-action's reward [40]; second, the complexity of combining super-actions increases exponentially with the number of single actions, which is not tractable.

We design the reward for a single action  $k \in \mathcal{K}$  in  $\text{SU}_t$  as

$$r_t = \begin{cases} \bar{\rho}_k(t) & \text{if } \chi(k, t) = 0; \\ -1 & \text{if } \chi(k, t) = 1, \end{cases} \quad (9)$$

where  $\bar{\rho}_k(t) \in [0, 1]$  represents the total number of bytes that can be sent during  $\text{SU}_t$  using channel  $k$ , normalized by the maximum number of bytes that can be sent when using the maximum modulation order, and  $\chi(k, t) \in \{0, 1\}$  indicates whether a collision happens using channel  $k$  during  $\text{SU}_t$ . As such, the reward in Eq. (9) is a function of both the channel and the resource allocation policies of all the agents. Furthermore, based on the assumption in Eq. (3), we have that the average reward of super-action  $\theta$  is the sum of the single average rewards, i.e.,

$$\mu(s, \theta) = \sum_{k \in \theta} \langle \phi_{\omega^*}(s), \beta_k \rangle, \forall s \in \mathcal{S}, \forall \theta \in \Theta, \quad (10)$$

where we assume that there exists a DNN  $\omega^* \in \Omega$  that provides the exact non-linear representation of the context  $s$ ,  $\forall s \in \mathcal{S}$ . The reward in Eq. (10) leads to a particular case of MA-CC-MAB referred to as *matroid bandits* [41]. In this case, it is possible to estimate the average reward obtained by super-action  $\theta$  as the sum of the estimated average rewards of all its base actions.

Based on the above introduction, we extend NLTS into the proposed DISNETS algorithm so that the agent can play super-action  $\theta_t$  in  $\text{SU}_t$  based on the following criteria:

- 1) Sample  $K$  vectors  $\{\hat{\beta}_k\}_{k=1}^K$  as described in Sec. V-B;
- 2) Compute the non-linear representation of the context, i.e.,  $\phi_\omega(s_t)$ , based on the context  $s_t$  at  $\text{SU}_t$ ;
- 3) Take super-action  $\theta_t = \{k \in \mathcal{K} : \phi_\omega(s_t)^T \beta_k > \epsilon\}$ , i.e., the agent transmits using all the orthogonal channels whose estimated reward (which is an indication of the transmission data rate) is larger than  $\epsilon$ .

Consequently, the average number of orthogonal channels that an agent can use is not constant, but rather learned

TABLE I: Simulation parameters.

Parameter	Value
Carrier frequency ( $f_c$ )	3.5 GHz
Overall system bandwidth ( $B$ )	60 MHz
5G protocol stack header ( $H$ )	72 bytes [42]
Subcarrier spacing ( $\Delta f$ )	60 kHz
SNR threshold ( $\text{SNR}_{\text{th}}$ )	-5 dB
Latency threshold ( $L_{\text{th}}$ )	1 ms
Noise temperature ( $T_B$ )	290 K
Antenna gain ( $G_{\text{UE}} = G_{\text{gNB}}$ )	0 dB
UE (UL) transmit power ( $P_{\text{TX,UL}}$ )	23 dBm
gNB (DL) transmit power ( $P_{\text{TX,DL}}$ )	30 dBm
Processing time at the UE ( $T_P$ )	7 OFDM symbols
Processing time at the UE ( $T_{\text{gNB}}$ )	7 OFDM symbols
5GC delay ( $T_{\text{CN}}$ )	0.1 ms
DAS delay ( $T_{\text{DAS}}$ )	0.05 ms
Length of the factory floor ( $l$ )	20 m [37]
Width of the factory floor ( $w$ )	20 m
Height of the factory floor ( $h$ )	4 m
Inter-machine distance ( $D$ )	5 m
Side of the machine ( $S$ )	3 m
Number of production lines ( $W$ )	4
Number of machines ( $M$ )	4/line
Inter-machine activation period $\tau_a$	8 ms
Packet size ( $Z_p$ )	616 Bytes
Simulation time ( $T_S$ )	7 s

and adjusted via DISNETS given the reward history and the context at time  $t$ . In addition, we further introduced a variance decaying factor  $\gamma$  to scale the sampling variance of the reward  $\nu_k(t)$  by  $\gamma$ , in order to force DISNETS to become more deterministic as the training progresses.

**Summary : DISNETS**

*Objective.* Compute the non-linear representation of the context  $\phi_\omega(s)$ , and choose a super-action  $\theta_t \in \mathcal{K}$  which returns the set of orthogonal channels that each UE should use to transmit data.

VI. NUMERICAL RESULTS

In Sec. VI-A we present our simulation parameters, in Sec. VI-B we show the convergence performance of DISNETS, and in Secs. VI-C and VI-D we evaluate the performance of DISNETS against some other benchmarks in terms of overhead, latency, and reliability.

A. Simulation Parameters

Simulation parameters are reported in Table I.

a) *System parameters:* The system operates with a carrier frequency of  $f_c = 3.5$  GHz and a bandwidth of  $B = 60$  MHz. We set 3GPP NR numerology 2 (i.e., a subcarrier spacing of  $\Delta_f = 60$  KHz), which leads to 84 RBs [43]. For the latency in Eq. (2), according to the 5G standard specifications we assume that (i) the processing times  $T_P$  and  $T_{\text{gNB}}$  at the UEs and the gNB, respectively, are both equal to 7 OFDM symbols, (i.e., 116.9  $\mu$ s for numerology 2), (ii) the propagation time  $\tau_P$  is neglected because it can be compensated with an accurate timing advance technique (see [44]), and (iii)  $\tau_F$  is also neglected due to its minor impact on  $L$ .

TABLE II: Structure of the DNN used in the DISNETS algorithm.

	Type	Size	Max Pool	Activation
Layer 1	Conv.	(10, 4, 4)	(3, 3)	Leaky ReLu
Layer 2	Conv.	(10, 3, 3)	(3, 3)	Leaky ReLu
Latent Layer	Linear	10	.	Leaky ReLu
Output Layer	Linear	$K$	.	Identity
Variance decaying factor ( $\gamma$ )			0.9999	
Number of optimization steps ( $O$ )			100	

b) *DISNETS parameters:* The configuration of the DNN used in DISNETS to compute the non-linear context representation is reported in Table II. Specifically, we consider two convolutional layers of size  $(\xi_1, \xi_2, \xi_3)$ , where  $\xi_1$  is the number of channels, and  $\xi_2$  and  $\xi_3$  are the kernel width and height, respectively, while the Max Pool field represents the size of the max pooling window. The dimension of the Latent Layer is set to 10. The size of the Output Layer is equal to the number of feasible single actions, i.e., orthogonal channels,  $K$ . The variance decaying factor is  $\gamma = 0.9999$ , and number of steps between two network updates (see Algorithm 1, line 10) is equal to  $O = 100$ . DISNETS' DNN implements the *Leaky Rectified Linear Unit (Leaky ReLu)* activation function.

c) *Performance metrics:* Numerical results are given in terms of the overhead (measured as the impact of FCI transmissions on the control channel), and the E2E latency and reliability defined in Sec. III-D, as a function of the number of UEs and the type of traffic.

d) *Benchmarks:* The performance of DISNETS is compared against the following baselines:

- GBS: it implements the standard centralized 5G NR GBS [15], which requires UEs and the gNB to exchange scheduling requests (via the PUCCH) and grants (via the PDCCCH), respectively, before transmitting data. In this case resource allocation is based on the number and size of packets that the UEs have in their queues when transmitting scheduling requests via the PUCCH.
- SPS: it implements the standard centralized 5G NR SPS [16], in which the gNB allocates (part of) the resources to the UEs semi-statically over a certain time interval. This approach promotes lower latency as resources are assigned only when UEs generate packets, and without additional message exchanges during transmission.
- NLTS: it implements distributed resource allocation based on the NLTS algorithm proposed in [22] and described in Sec. V-B(b), thus with the assumption that UEs can transmit through one single orthogonal channel.
- RandomK: it implements distributed resource allocation, in which UEs use exactly  $K^*$  orthogonal channels (i.e., RBs) for each of their packet transmissions, and  $K^*$  is optimized via exhaustive search. Notice that RandomK is not state-of-the-art, but has been explicitly proposed, designed, and implemented to have another decentralized benchmark to compare the performance of DISNETS.

B. Training Convergence

First, we study the training performance of the proposed DISNETS framework considering uniformly aperiodic traffic,

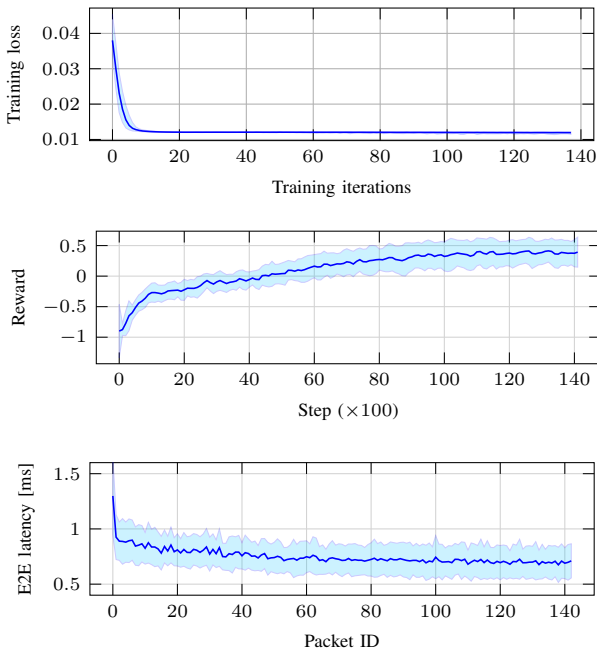
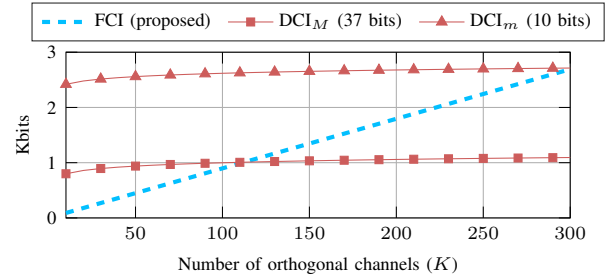


Fig. 3: Convergence performance of DISNETS in terms of empirical average and standard deviation of the training loss (top), reward (center), and E2E latency (bottom). We consider uniformly aperiodic traffic, with  $t_{min} = 2$  ms,  $t_{max} = 6$  ms, and  $N = 60$ .

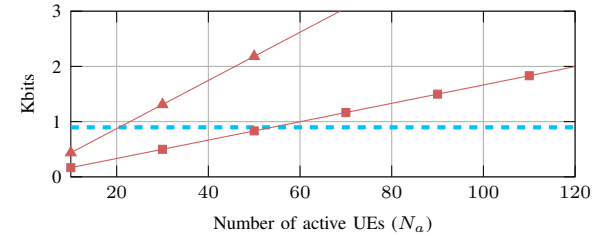
with  $t_{min} = 2$  ms,  $t_{max} = 6$  ms, and  $N = 60$  UEs. Fig. 3 (top) plots the average and standard deviation of the training loss of the NLTS module of DISNETS (specifically, the DNN), which is used to learn the non-linear representation of the context  $\phi_\omega(s)$ . The loss decreases quite quickly, and becomes stable after around 0.5 s, which is an indication of the accuracy of the DISNETS implementation. In fact, as the training progresses, UEs are learning to allocate resources more accurately.

In Fig. 3 (center) we plot the statistics of the reward obtained by the agents as a function of the total number of interactions with the environment. We can see that, at the beginning, the reward is close to  $-1$  given that all UEs start making random decisions in terms of the orthogonal channels to use at each SU. Then, the average reward is an increasing function of the number of steps, meaning that the UEs are learning to make more accurate allocations as the training progresses. Interestingly, we can recognize two training phases. At first the UEs are learning fast, at the rate of convergence of the DNN: in this phase, the average reward increases steeply. This is motivated by the fact that, at the beginning of the training phase, many collisions occur, which gives DISNETS more chances to optimize based on the relative rewards. Then, DISNETS takes more time to achieve better cooperation, and the framework optimizes more slowly.

In Fig. 3 (bottom) we plot the statistics of the E2E latency experienced by the UEs as a function of the packet ID. Again, it is possible to separate the two training regimes. At first, DISNETS can estimate the number of orthogonal channels to use to minimize collisions starting from a random guess, and achieves an average latency of around 1 ms. Then, DISNETS is used to further optimize resource allocation reducing the latency to around 0.7 ms, though taking more time to converge.



(a) Impact of the number of channels. We set  $N_a = 60$  and  $N = 500$ .



(b) Impact of the number of active UEs. We set  $N = 500$  and  $K = 100$ .

Fig. 4: Overhead performance measured in terms of the size of the FCI (proposed) vs. the 3GPP NR DCI, as a function of the number of orthogonal channels (top) and UEs (bottom). We consider two DCI formats, namely DCI<sub>m</sub> and DCI<sub>M</sub>, which require up to 10 and 37 additional bits, respectively, for resource allocation [23].

### C. Overhead

As described in Sec. V-A, DISNETS requires periodic FCI transmissions, which include the transmission outcomes (successful transmission, collision, or outage) relative to every UE on each orthogonal channel, and is used to generate the context and the reward. Therefore, the size of the FCI (in bits) can be computed as  $K \cdot \log_2(N + 3)$  (see Table III).

The structure of the FCI is similar to that of the 5G NR DCI signal [23], which is used to handle downlink transmissions. The size of the DCI depends on the number of orthogonal channels  $K$ . Moreover, while the FCI embeds information for all UEs, the DCI is transmitted only to the *active* UEs  $N_a \subseteq N$ , so the overall size (in bits) goes as  $N_a \cdot \log_2(K)$ . Furthermore, the DCI requires an additional (variable) number of bits to carry information for, e.g., carrier aggregation, HARQ, frequency allocation, channel access [23, Sec. 10.1.4]. 3GPP NR defines 10+ different DCI formats. For simplicity, we consider two representative DCI formats, namely DCI<sub>m</sub> and DCI<sub>M</sub>, which require 10 and 37 additional bits, respectively, and the relative DCI size is reported in Table III.

Based on the above introduction, in Fig. 4 we plot the size of the FCI, DCI<sub>m</sub>, and DCI<sub>M</sub> signals, which is directly proportional to the overhead. Specifically, we see that the size of the FCI scales linearly with the number of orthogonal

TABLE III: Size (in bits) of the FCI and DCI signals, vs. the number of active UEs ( $N_a$ ) and the number of orthogonal channels ( $K$ ). The total number of UEs in the system is set to  $N = 500$ .

FCI	DCI	
	DCI <sub>m</sub>	DCI <sub>M</sub>
$K \cdot \log_2(N + 2)$	$N_a \cdot (\log_2 K + 10)$	$N_a \cdot (\log_2 K + 37)$

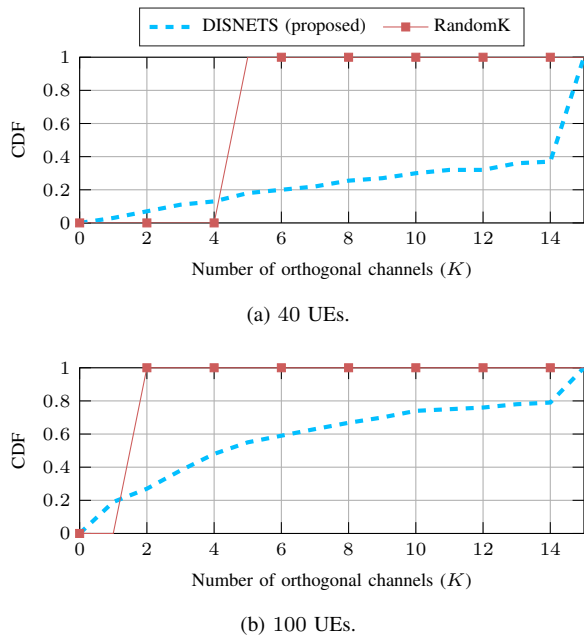


Fig. 5: Empirical CDF of the number of orthogonal channels used at each scheduling opportunity relative to the last 10 packets considering DISNETS vs. RandomK, as a function of the number of UEs.

channels (Fig. 4a) and logarithmically with the number of active UEs (Fig. 4b), while for the DCI it is almost the opposite. As such, DISNETS achieves comparable or lower overhead than other solutions based on the DCI (e.g., 5G NR GBS) in many reasonable configurations. Notice that the results in Fig. 4 do not account for the additional overhead introduced to send (receive) scheduling requests (grants) in GBS, which is not required in DISNETS since resource allocation is distributed.

As another measure of overhead, in Fig. 5 we plot the empirical Cumulative Distribution Function (CDF) of the number of orthogonal channels used at each scheduling opportunity for DISNETS vs. RandomK, which is an indication of the channel occupancy. Statistics are referred to the last 10 packets, i.e., after the convergence of DISNETS. We observe that RandomK uses a constant (though optimized) number of channels per UE equal to  $K^* \in \{5, 2\}$  for  $N \in \{40, 100\}$  respectively, so  $K^*$  is a decreasing function of  $N$ . This is due to the fact that, as the number of UEs increases, the number of collisions also increases: in these conditions, the system is encouraged to reduce the number of channels to reduce the probability of collision. On the other hand, the adaptability and flexibility features of DISNETS make the number of channels to use for transmission vary significantly; as such, UEs are free to optimize the number of resources as a function of  $N$ . Notice that, even though RandomK uses on average less resources than DISNETS, it results in more collisions (see Figs. 6 and 7), which would increase the number of re-transmissions and, eventually, the overall number of resources. Eventually, the performance of RandomK (in terms of latency and reliability) is worse than that of DISNETS because RandomK is unable to optimize.

#### D. Performance Evaluation

a) *Impact of the number of UEs and the resource allocation strategy:* We now compare the performance of DISNETS against those of RandomK, NLTS, GBS, and SPS baselines as a function of the number of UEs in the system. Fig. 6a reports the E2E latency considering uniformly aperiodic traffic. As expected, the E2E latency increases as  $N$  increases given that the network is more congested, which increases the probability of collision and re-transmissions. Also, we can see that DISNETS always outperforms all the benchmarks. In particular, centralized GBS is not able to satisfy the  $L_{th} = 1$  ms requirement of URLLC due to the additional delays introduced to send (receive) scheduling requests (grants), especially when the number of UEs increases. Interestingly, GBS outperforms SPS in case of aperiodic traffic. In fact, SPS is designed to work well as long as the traffic is periodic [11]: in this case, SPS can pre-allocate resources based on the actual traffic periodicity, and does not require the UEs and the gNB to exchange additional messages. However, for aperiodic traffic as in Fig. 6, SPS may not be able to react to possible (unpredictable) changes in the traffic patterns and requests, with respect to how resources were originally pre-assigned, which implies that the system may operate in a sub-optimal configuration [45]. As such, unscheduled UEs will keep data packets in the queue, thus accumulating delays, at least until SPS is re-configured by another RRC interaction.

Compared to another distributed benchmark such as RandomK, DISNETS can reduce the E2E latency by up to 20%. In fact, DISNETS exploits coordination, and is designed to optimize resource allocation depending on the type of traffic and the relative load of machines (for example allocating more resources to machines with more UEs). In the end, the latency for NLTS is up to  $1.71\times$  and  $2\times$  higher than DISNETS and RandomK, respectively, given that UEs can use only one orthogonal channel. While this approach brings the probability of collision to almost zero, it leaves the network underutilized. In comparison, RandomK uses  $K^*$  channels, while DISNETS can dynamically adapt the number of channels to optimize the trade-off between latency and collision.

Moreover, in Fig. 6b we consider the case of UE-specific aperiodic traffic. We observe that DISNETS and GBS can exploit the additional degrees of correlation introduced in the traffic to improve the latency compared to Fig. 6a. This is particularly true for  $N \leq 80$ , while for  $N > 80$  the performance degrades quickly due to congestion. Still, DISNETS is the only scheme able to satisfy the  $L_{th} = 1$  ms latency requirement in all configurations as it learns more from the correlation in the packet generation process. Notice that the latency for RandomK and SPS is slightly higher than in the scenario in Fig. 6a due to the fact that the extra packets generated in the interval  $[t_{min}, t_{max}]$  may create more collisions. A similar observation holds for the NLTS baseline.

We recall that URLLC requires both low latency and high reliability. In Sec. III-D we defined reliability  $\eta_t(L_{th})$  as the probability that the E2E latency associated with a packet is below a pre-defined requirement (here set to  $L_{th} = 1$  ms). To capture this trend, in Fig. 7 we plot the probability density function (pdf) (top) and CDF (bottom) of the E2E latency for DISNETS vs. RandomK (the two best solutions for resource

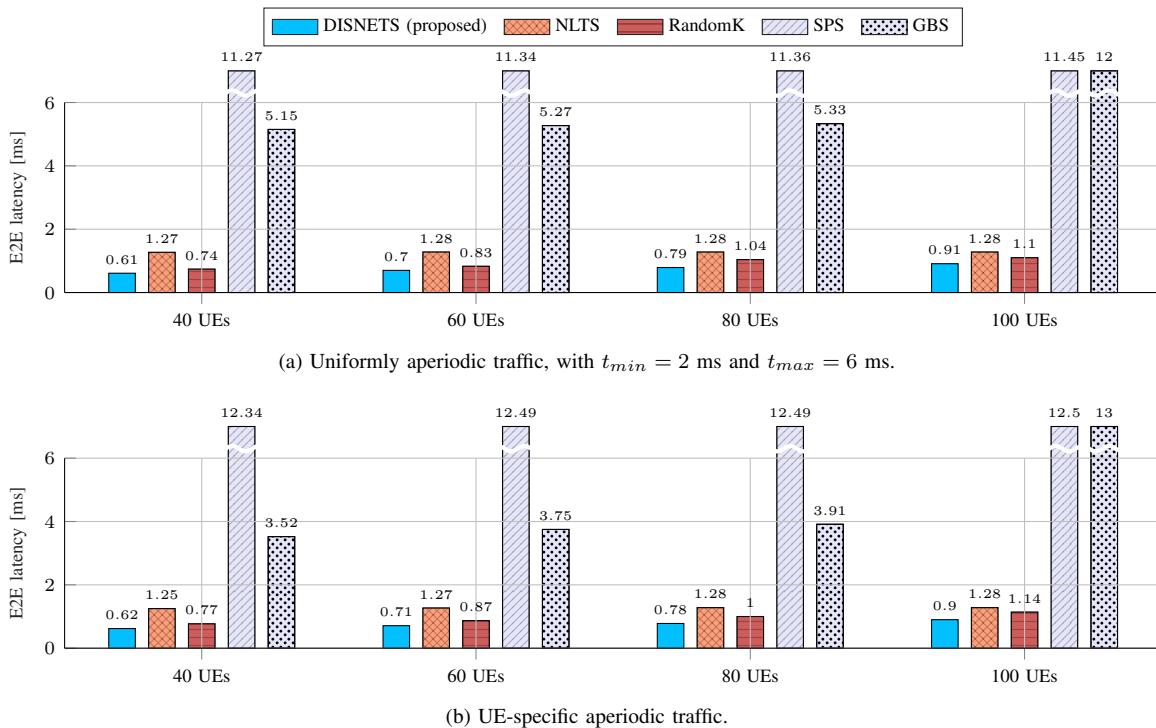


Fig. 6: Average E2E latency for DISNETS vs. RandomK, NLTS, SPS, and GBS, as a function of the number of UEs and the type of traffic.

allocation based on the previous results). We can see that the latency distributions for DISNETS are strongly shifted towards the left compared to RandomK (an indication of a smaller E2E latency), and the gap increases as  $N$  increases. For example, while for  $N = 40$  (Fig. 7a) both systems achieve comparable performance, for  $N = 100$  (Fig. 7c) we have that only 46% of the UEs experience an E2E lower than  $L_{th} = 1$  ms using RandomK, vs. 80% for DISNETS.

*b) Impact of the type of traffic:* From the previous paragraphs we concluded that SPS and NLTS are not compatible with URLLC requirements for aperiodic traffic. So, in this set of experiments we focus on DISNETS, RandomK, and GBS as a function of the type of traffic. First, in Fig. 8 we change the value of  $t_{min}$ , which is inversely proportional to the traffic load, considering both uniformly aperiodic (Fig. 8a) and UE-specific aperiodic traffic (Fig. 8b). We can see that DISNETS is better than any other benchmark, and the latency is consistently below 1 ms in all configurations. Notice that for GBS the E2E latency increases as  $t_{min}$  decreases because the traffic is more intense and the system is more congested. On the contrary, for RandomK and DISNETS we have the opposite trend, i.e., the E2E latency increases as  $t_{min}$  increases. This is motivated by the fact that, as  $t_{min}$  approaches  $t_{max} = 6$  ms, the traffic becomes quasi-deterministic and the UEs tend to generate packets almost simultaneously, which may increase the number of collisions. Consequently, achieving coordination becomes harder. Still, for DISNETS the latency grows as little as 7%, from 0.7 for  $t_{min} = 1$  ms to 0.75 ms for  $t_{min} = 5$  ms. In turn, the performance of RandomK deteriorates significantly as  $t_{min}$  increases, and almost achieves the same performance as GBS in the long term.

Finally, in Fig. 9 we study the E2E latency as a function of the percentage of aperiodic UEs in the network. Specifically,

for the fraction of aperiodic UEs we set  $t_{min} = 2$  ms and  $t_{max} = 6$  ms, whereas for the periodic UEs we set  $\tau = 2$  ms. As such, the average inter-packet interval for aperiodic UEs is equal to 4 ms vs. 2 ms for periodic UEs, which means that the latter generates more traffic. Again, we see that DISNETS outperforms the other benchmarks, and is therefore able to work well in both periodic and mixed, i.e., periodic and aperiodic, traffic conditions. Notably, the performance of GBS decreases as the traffic becomes more aperiodic. This is expected, and we proved in [11], [45] that GBS, as well as SPS, do not work well in case of unpredictable aperiodic traffic. For example, in case of GBS, some packets may be generated towards the end of an activation period, and cannot send scheduling requests within the current activation period, so packets remain in the queue and accumulate delay. On the other hand, as mentioned in Fig. 8, DISNETS and RandomK have the opposite trend, and suffer more when the traffic becomes periodic given that periodic UEs generate more traffic than aperiodic UEs. Still, DISNETS is able to converge to good and stable results, and decrease the latency by up to 86% and 50% compared to GBS and RandomK, respectively.

*c) DISNETS vs. RandomK:* The above results demonstrate the superior performance of DISNETS compared to RandomK under several metrics. For example, for 100 UEs, DISNETS can reduce the latency by up to 20% (see Fig. 6), and improve reliability by up to 40% (see Fig. 8). Moreover, RandomK requires offline simulations to identify the optimal value of  $K$ , i.e.,  $K^*$  (since  $K^*$  changes as changing the traffic periodicity and the number of UEs), which may be time consuming and not always feasible in practice. On the other hand, DISNETS is flexible enough to adapt to different scenarios after the training phase (which is done only once).

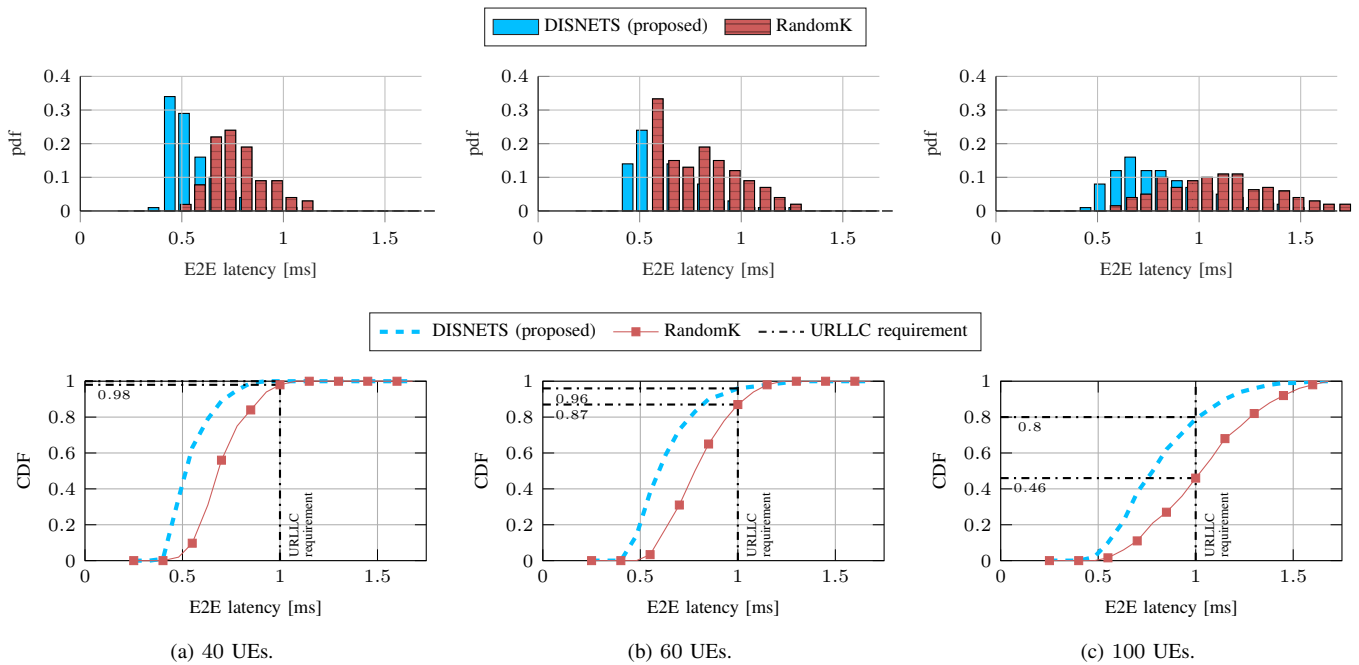


Fig. 7: Empirical pdf (top) and CDF (bottom) of the E2E latency considering DISNETS vs. RandomK as a function of the number of UEs. We consider uniformly aperiodic traffic, with  $t_{min} = 2$  ms and  $t_{max} = 6$  ms.

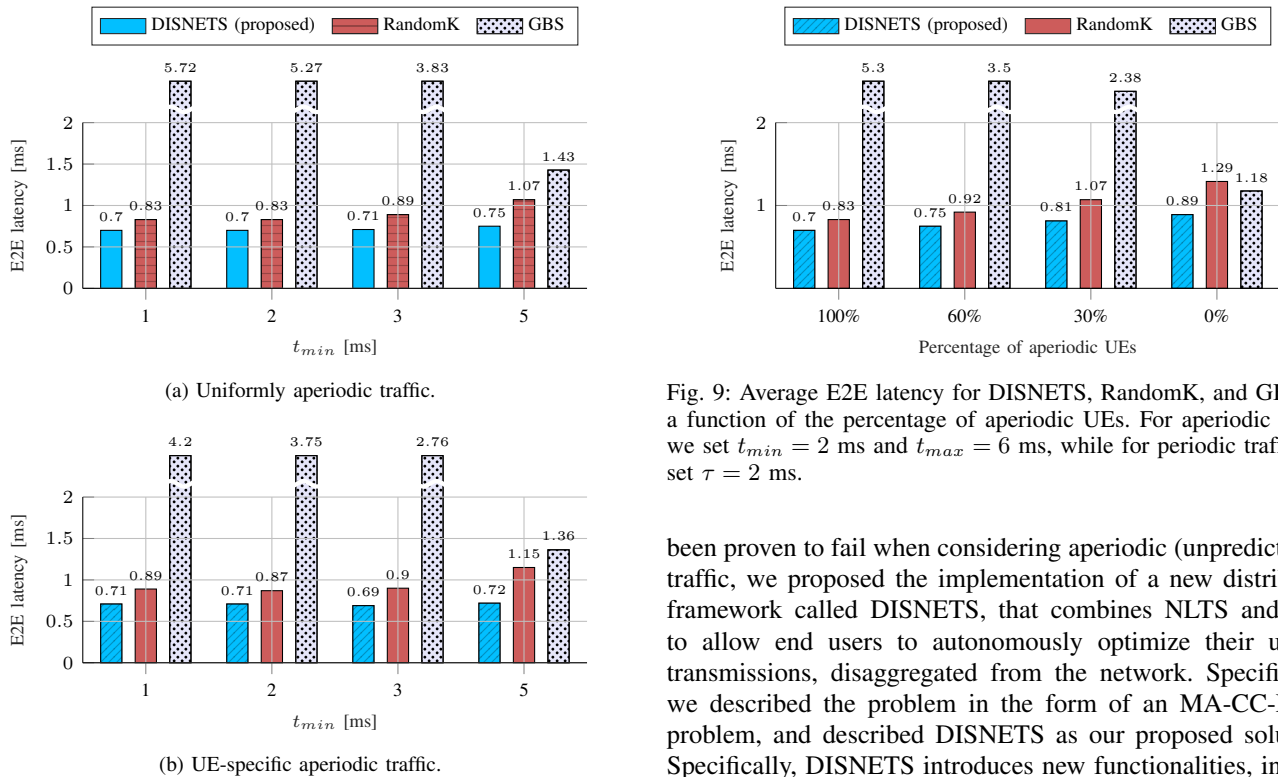


Fig. 8: Average E2E latency for DISNETS, RandomK, and GBS, as a function of  $t_{min}$  and the type of traffic. We set  $t_{max} = 6$  ms.

VII. CONCLUSION AND FUTURE WORK

In this paper we shed light on the issue of enabling URLLC in IIoT networks. Specifically, we focused on the impact of resource allocation on the E2E latency. While the two main 5G NR centralized schedulers, namely GBS and SPS, have

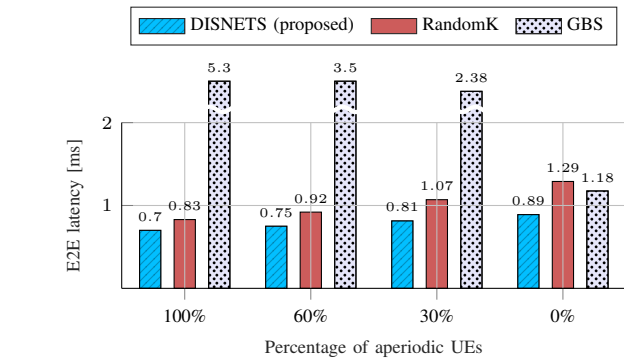


Fig. 9: Average E2E latency for DISNETS, RandomK, and GBS, as a function of the percentage of aperiodic UEs. For aperiodic traffic we set  $t_{min} = 2$  ms and  $t_{max} = 6$  ms, while for periodic traffic we set  $\tau = 2$  ms.

been proven to fail when considering aperiodic (unpredictable) traffic, we proposed the implementation of a new distributed framework called DISNETS, that combines NLTS and LTS to allow end users to autonomously optimize their uplink transmissions, disaggregated from the network. Specifically, we described the problem in the form of an MA-CC-MAB problem, and described DISNETS as our proposed solution. Specifically, DISNETS introduces new functionalities, including (i) a new control signaling scheme called FCI to train the DISNETS framework, and (ii) a new protocol procedure for autonomously selecting multiple radio resources to reduce the probability of collision. We showed via simulations that DISNETS is compatible with URLLC even for aperiodic traffic and considering IIoT-specific correlations, and outperforms state-of-the-art centralized and decentralized benchmarks.

As part of our future work, we plan to develop a scalable and practical demonstrator using 5G off-the-shelf commercial

equipment to emulate distributed resource allocation for IIoT URLLC based on the studies of this paper.

## REFERENCES

- [1] M. Giordani, M. Polese, M. Mezzavilla, S. Rangan, and M. Zorzi, "Toward 6G Networks: Use Cases and Technologies," *IEEE Communications Magazine*, vol. 58, no. 3, pp. 55–61, Mar. 2020.
- [2] M. Wollschlaeger, T. Sauter, and J. Jasperneite, "The future of industrial communication: Automation networks in the era of the internet of things and industry 4.0," *IEEE Industrial Electronics Magazine*, vol. 11, no. 1, pp. 17–27, Mar. 2017.
- [3] J. Cheng, W. Chen, F. Tao, and C.-L. Lin, "Industrial IIoT in 5G environment towards smart manufacturing," *Journal of Industrial Information Integration*, vol. 10, pp. 10–19, Jun. 2018.
- [4] S. Vitturi, C. Zunino, and T. Sauter, "Industrial communication systems and their future challenges: Next-generation Ethernet, IIoT, and 5G," *Proceedings of the IEEE*, vol. 107, no. 6, pp. 944–961, May 2019.
- [5] J. Lee, B. Bagheri, and H.-A. Kao, "A Cyber-Physical Systems architecture for Industry 4.0-based manufacturing systems," *Manufacturing Letters*, vol. 3, pp. 18 – 23, Jan. 2015.
- [6] 5G-ACIA, "5G for Automation in Industry: Primary use cases, functions and service requirements," *White Paper*, 2019.
- [7] 3GPP, "Service requirements for cyber-physical control applications in vertical domains; Stage 1 (Release 18)," *TS 22.104*, 2021.
- [8] J. Oueis and E. C. Strinati, "Uplink traffic in future mobile networks: Pulling the alarm," in *International Conference on Cognitive Radio Oriented Wireless Networks (CROWNCOM)*, 2016.
- [9] N. Patriciello, S. Lagen, L. Giupponi, and B. Bojovic, "The Impact of NR scheduling timings on end-to-end delay for uplink traffic," in *IEEE Global Communications Conference (GLOBECOM)*, 2019.
- [10] L. Liang, H. Ye, and G. Y. Li, "Spectrum sharing in vehicular networks based on multi-agent reinforcement learning," *IEEE Journal on Selected Areas in Communications*, vol. 37, no. 10, pp. 2282–2292, Aug. 2019.
- [11] G. Cuzzo, S. Cavallero, F. Pase, M. Giordani, J. Eichinger, C. Buratti, R. Verdone, and M. Zorzi, "Enabling URLLC in 5G NR IIoT Networks: A Full-Stack End-to-End Analysis," in *Joint European Conference on Networks and Communications & 6G Summit (EuCNC/6G Summit)*, 2022.
- [12] 3GPP, "NR and NG-RAN Overall Description (Release 15)," *TS 38.300*, 2018.
- [13] A. Larrañaga, M. C. Lucas-Estañ, I. Martínez, and J. Gozalvez, "5G NR Configured Grant in ns-3 Network Simulator for Ultra-Reliable Low Latency Communications," *Procedia Computer Science*, vol. 201, pp. 495–502, Mar. 2022.
- [14] X. Lin, J. Li, R. Baldemair, J.-F. T. Cheng, S. Parkvall, D. C. Larsson, H. Koorapaty, M. Frenne, S. Falahati, A. Grovlen *et al.*, "5G new radio: Unveiling the essentials of the next generation wireless access," *3GPP, "Evolved Universal Terrestrial Radio Access (E-UTRA); Physical layer procedures," TS 36.213*, 2021.
- [15] —, "Semi-Persistent Scheduling for 5G New Radio URLLC," *R1-167309*, 2016.
- [16] Y. Liu, Y. Deng, M. ElKashlan, A. Nallanathan, and G. K. Karagiannidis, "Analyzing grant-free access for URLLC service," *IEEE Journal on Selected Areas in Communications*, vol. 39, no. 3, pp. 741–755, Mar. 2020.
- [17] A. T. Z. Kasgari and W. Saad, "Model-Free Ultra Reliable Low Latency Communication (URLLC): A Deep Reinforcement Learning Framework," in *IEEE International Conference on Communications (ICC)*, 2019.
- [18] A. Slivkins, "Introduction to Multi-Armed Bandits," *Foundations and Trends® in Machine Learning*, vol. 12, 2019.
- [19] D. J. Russo, B. V. Roy, A. Kazerouni, I. Osband, and Z. Wen, "A tutorial on Thompson Sampling," *Foundations and Trends in Machine Learning*, vol. 11, no. 1, 2018.
- [20] F. Pase, M. Giordani, G. Cuzzo, S. Cavallero, J. Eichinger, R. Verdone, and M. Zorzi, "Distributed Resource Allocation for URLLC in IIoT Scenarios: A Multi-Armed Bandit Approach," *IEEE GLOBECOM Workshops (GC Wkshps)*, 2022.
- [21] C. Riquelme, G. Tucker, and J. Snoek, "Deep Bayesian Bandits Showdown," *International Conference on Learning Representations (ICLR)*, 2018.
- [22] S. Parkvall, E. Dahlman, and J. Sköld, *5G NR: The Next Generation Wireless Access Technology*. Academic Press, 2018.
- [23] —, "technology," *IEEE Communications Standards Magazine*, vol. 3, no. 3, pp. 30–37, Sep. 2019.
- [24] M. Bennis, M. Debbah, and H. V. Poor, "Ultrareliable and low-latency wireless communication: Tail, risk, and scale," *Proceedings of the IEEE*, vol. 106, no. 10, pp. 1834–1853, Sep. 2018.
- [25] X. Jiang, H. Shokri-Ghadikolaei, G. Fodor, E. Modiano, Z. Pang, M. Zorzi, and C. Fischione, "Low-latency networking: Where latency lurks and how to tame it," *Proceedings of the IEEE*, vol. 107, no. 2, pp. 280–306, Aug. 2018.
- [26] H. Ren, C. Pan, Y. Deng, M. ElKashlan, and A. Nallanathan, "Resource Allocation for URLLC in 5G Mission-Critical IoT Networks," in *IEEE International Conference on Communications (ICC)*, 2019.
- [27] C. She, R. Dong, Z. Gu, Z. Hou, Y. Li, W. Hardjawana, C. Yang, L. Song, and B. Vucetic, "Deep Learning for Ultra-Reliable and Low-Latency Communications in 6G Networks," *IEEE Network*, vol. 34, no. 5, pp. 219–225, Jul. 2020.
- [28] A. Azari, M. Ozger, and C. Cavdar, "Risk-Aware Resource Allocation for URLLC: Challenges and Strategies with Machine Learning," *IEEE Communications Magazine*, vol. 57, no. 3, pp. 42–48, Mar. 2019.
- [29] Z. Gu, C. She, W. Hardjawana, S. Lumb, D. McKechnie, T. Essery, and B. Vucetic, "Knowledge-Assisted Deep Reinforcement Learning in 5G Scheduler Design: From Theoretical Framework to Implementation," *IEEE Journal on Selected Areas in Communications*, vol. 39, no. 7, pp. 2014–2028, May 2021.
- [30] F. Bragato, T. Lotta, G. Ventura, M. Drago, F. Mason, M. Giordani, and M. Zorzi, "Towards Decentralized Predictive Quality of Service in Next-Generation Vehicular Networks," *IEEE Information Theory and Applications Workshop (ITA)*, 2023. [Online]. Available: <https://arxiv.org/abs/2302.11268>
- [31] I. Bistriz, T. Z. Baharav, A. Leshem, and N. Bambos, "One for all and all for one: Distributed learning of fair allocations with multi-player bandits," *IEEE Journal on Selected Areas in Information Theory*, vol. 2, no. 2, pp. 584–598, Apr. 2021.
- [32] H. Ye and G. Y. Li, "Deep Reinforcement Learning based Distributed Resource Allocation for V2V Broadcasting," in *14th International Wireless Communications & Mobile Computing Conference (IWCMC)*, 2018.
- [33] 5G-Clarity, "Use Case Specifications and Requirements," *Verband der Elektro- und Digitalindustrie (ZVEI) White Paper*, Mar. 2020.
- [34] 5G-ACIA, "5G for Connected Industries and Automation," *Verband der Elektro- und Digitalindustrie (ZVEI) White Paper*, Feb. 2019.
- [35] 3GPP, "Study on channel model for frequencies from 0.5 to 100 GHz (Release 16)," *TR 38.901*, 2019.
- [36] —, "NR - Physical layer procedures for data (Release 15)," *TS 38.214*, 2018.
- [37] 5G-ACIA, "Integration of Industrial Ethernet Networks with 5G networks," *Verband der Elektro- und Digitalindustrie (ZVEI) White Paper*, Nov. 2019.
- [38] L. Chen, J. Xu, and Z. Lu, "Contextual combinatorial multi-armed bandits with volatile arms and submodular reward," in *Advances in Neural Information Processing Systems (NeurIPS)*, 2018.
- [39] S. Agrawal and N. Goyal, "Thompson sampling for contextual bandits with linear payoffs," *International Conference on Machine Learning (ICML)*, 2013.
- [40] S. Wang and W. Chen, "Thompson sampling for combinatorial semi-bandits," *International Conference on Machine Learning (ICML)*, 2018.
- [41] B. Kveton, Z. Wen, A. Ashkan, H. Eydgahi, and B. Eriksson, "Matroid bandits: Fast combinatorial optimization with learning," *30th Conference on Uncertainty in Artificial Intelligence (UAI)*, 2014.
- [42] ETSI, "Study on 5G NR User Equipment (UE) application layer data throughput performance," *TR 137 901-5*, 2020.
- [43] 3GPP, "NR - Physical channels and modulation (Release 15)," *TS 38.211*, 2018.
- [44] —, "Study on NR Industrial Internet of Things (IIoT) (Release 16)," *TS 38.825*, 2019.
- [45] S. Cavallero, N. S. Grande, F. Pase, M. Giordani, J. Eichinger, C. Buratti, R. Verdone, and M. Zorzi, "A New Scheduler for URLLC in 5G NR IIoT Networks with Spatio-Temporal Traffic Correlations," in *IEEE International Conference on Communications (ICC)*, 2023.